





**Please cite the Published Version**

Pascual-García, A , Rivett, DW , Jones, Matt Lloyd  and Bell, T  (2025) Replicating community dynamics reveals how initial composition shapes the functional outcomes of bacterial communities. *Nature Communications*, 16 (1). 3002 ISSN 2041-1723

**DOI:** <https://doi.org/10.1038/s41467-025-57591-2>

**Publisher:** Springer

**Version:** Supplemental Material

**Downloaded from:** <https://e-space.mmu.ac.uk/639314/>

**Usage rights:**  [Creative Commons: Attribution 4.0](https://creativecommons.org/licenses/by/4.0/)

**Additional Information:** This is an open access article which first appeared in *Nature Communications*

**Data Access Statement:** Sequences associated with this study are deposited at NCBI under BioProject accession number PRJNA989519. This project contains the 16S rRNA amplicon sequencing data associated with each of the communities at day 0, as well as at day 7 for the four replicate growth experiments. Source data and additional processed data are also available in the Code repository with details to reproduce data and figures. Source data are provided with this paper. Code used for all the analysis presented in the manuscript was deposited in GitHub with the URL: <https://github.com/apascualgarcia/ReplayEcology>, and the first release was permanently stored in DOI: 10.5281/zenodo.13785758.

**Enquiries:**

If you have questions about this document, contact [openresearch@mmu.ac.uk](mailto:openresearch@mmu.ac.uk). Please include the URL of the record in e-space. If you believe that your, or a third party's rights have been compromised through this document please see our Take Down policy (available from <https://www.mmu.ac.uk/library/using-the-library/policies-and-guidelines>)

# Supplementary Materials

## Replicating community dynamics reveals reveals how initial composition shapes the functional outcomes of bacterial communities

A. Pascual-García<sup>(1,2,†)</sup>, D. Rivett<sup>(3,†)</sup>, M. L. Jones<sup>(4)</sup>, T. Bell<sup>(5,\*)</sup>

(1) Centro Nacional de Biotecnología, CSIC, Madrid, Spain

(2) Institute of Integrative Biology, ETH, Zürich, Switzerland

(3) Department of Natural Sciences, Faculty of Science and Engineering, Manchester Metropolitan University, Manchester, United Kingdom.

(4) Environment and Sustainability Institute, University of Exeter, Penryn, Cornwall, United Kingdom.

(5) Imperial College London, Silwood Park, Ascot, United Kingdom.

(†) Equal contribution

(\*) correspondence: thomas.bell@imperial.ac.uk

## Contents

<b>Supplementary Figures</b>	<b>2</b>
<b>Supplementary Text</b>	<b>5</b>
Supplementary Note 1. Identification of classes and statistical significance . . . . .	5
Supplementary Note 2. Landscape transformation and equivalent classes . . . . .	7
Supplementary Note 3. Relative abundances change of ASVs propensities' groups . . . . .	10
Supplementary Note 4. Statistical analysis of metagenomics predictions . . . . .	11
<b>References</b>	<b>14</b>

14

## Supplementary Figures

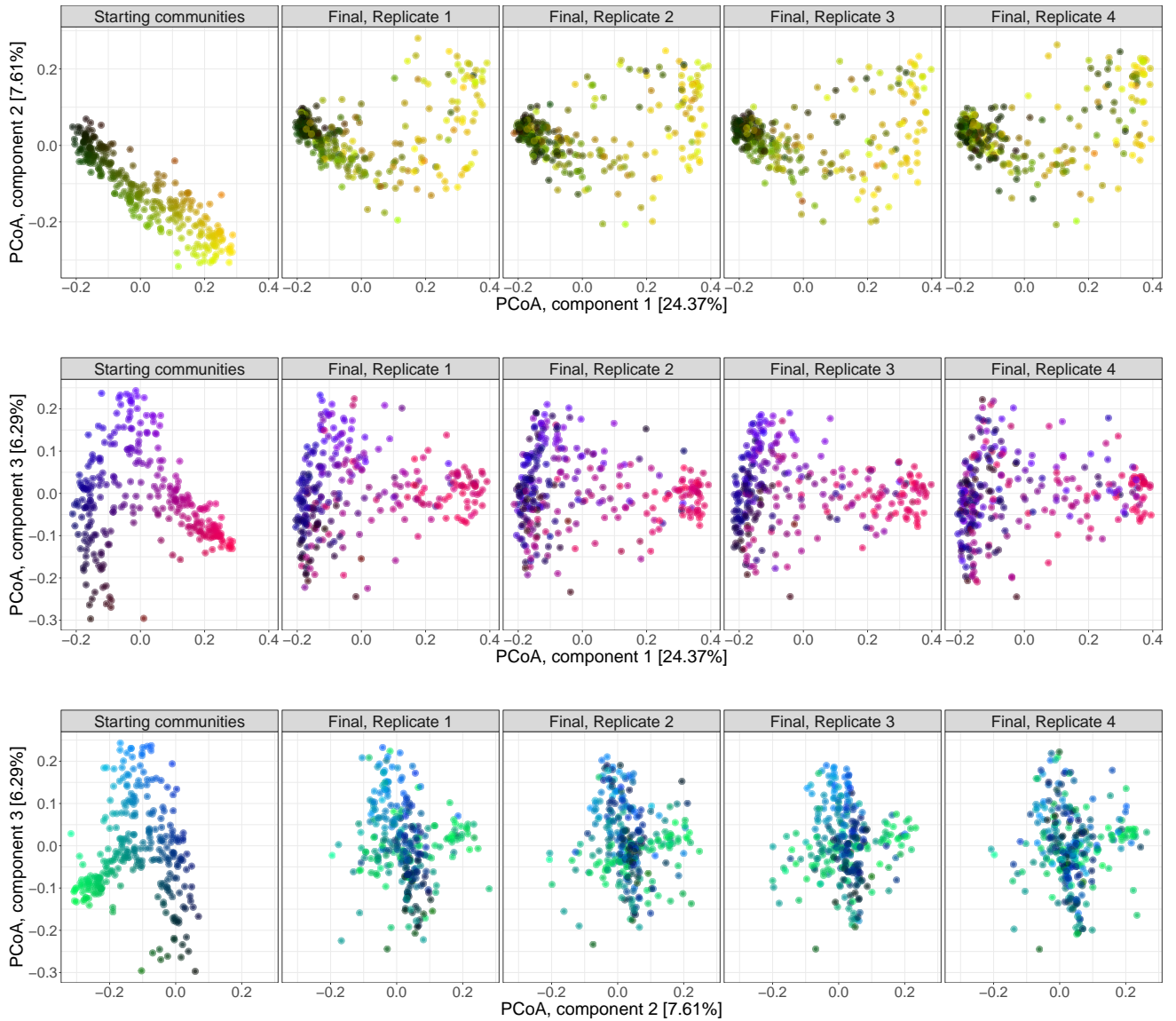


Figure 1: **Illustration of trajectories.** PCoA performed with the Jensen-Shannon divergence and projected on coordinates 1 and 2 (top), 1 and 3 (middle), and 2 and 3 (bottom), with the communities coloured by their starting position in the ordination space. Final replicates were split in different boxes for clarity.

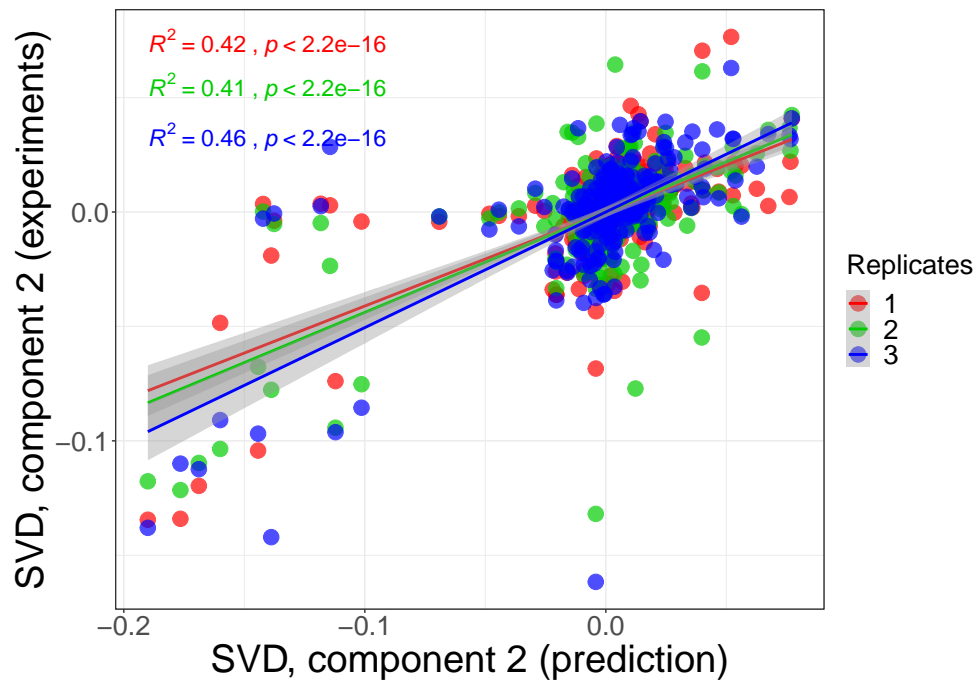


Figure 2: **Predicted final composition** of starting communities after rigid-body transformation against the composition of the replicates not used to find the transformation. The second Singular Value Decomposition component is used for the comparison.

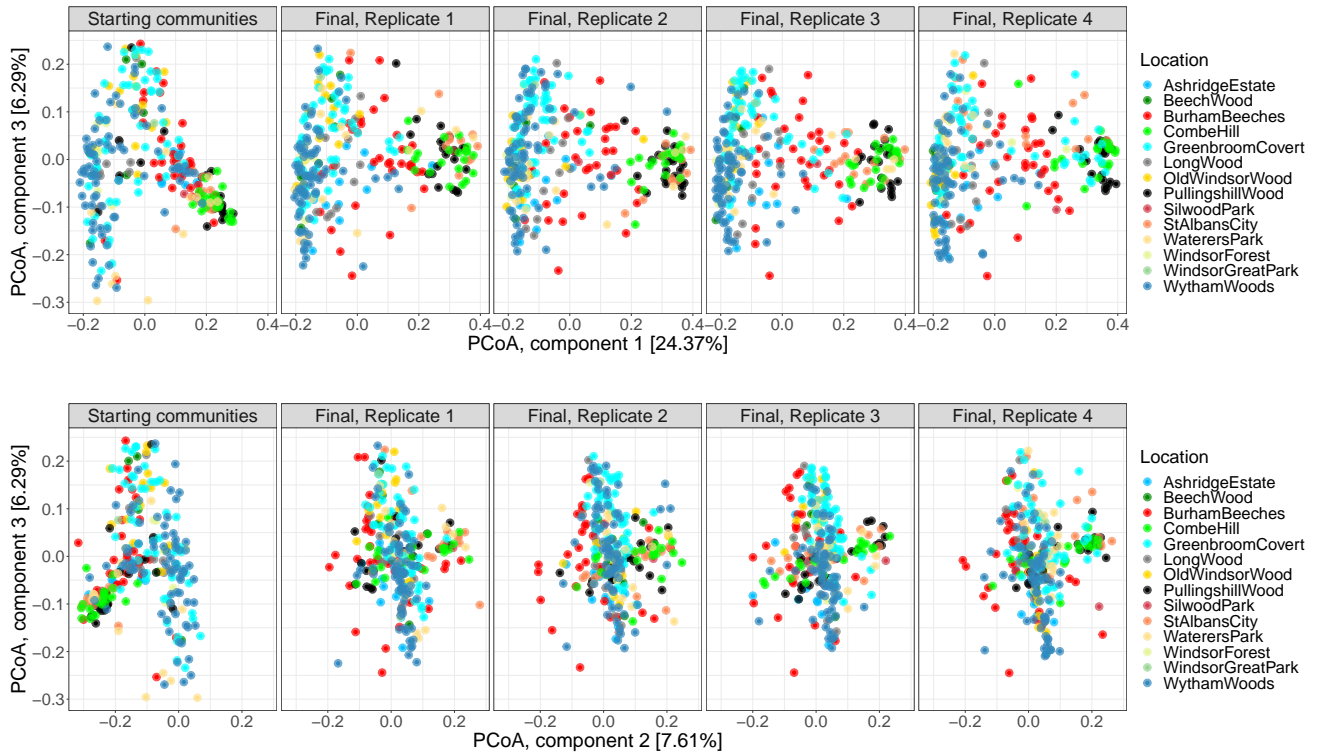


Figure 3: **History of communities.** PCoA performed with the Jensen-Shannon divergence and projected on coordinates 1 and 2 (top) and 1 and 3 (bottom), with the communities coloured by their location. Final replicates were split in different boxes for clarity.

## Supplementary Text

### Supplementary Note 1. Identification of classes and statistical significance

As indicated in the Main Text (see Methods) to identify the number of classes we performed a Partition Around Medoids clustering, which requires as an input the number of clusters  $k$ . To identify the optimal clustering, we computed the Calinski-Harabasz ( $CH$ ) index and chose the classification having the maximum value of this quantity, shown in Suppl. Fig. 4. In previous work, we followed a similar procedure but worked with just the starting communities and used Operational Taxonomix Units clustered at 97% sequence identity (see (1) for details), which resulted in six clusters (community classes). In this work, we found that working with Amplicon Sequence Variants the number of classes increased to 17 (see Suppl. Fig. 4, left) with a second maximum when the number of clusters was 6. For consistency with previous work we chose this second maximum as our reference classification, and we confirmed that both classifications were qualitative similar, allowing us to interpret our results at the light of previous findings. Only 5 classes were represented in the subset of starting communities that were resurrected in this study. For the final communities, the  $CH$  index becomes more skewed, dropping precipitously for any clustering beyond  $k = 2$ , suggesting that the compositional landscape was simplified with respect to the starting landscape (see Suppl. Fig. 4, right). Finally, the significance of the classes was evaluated by computing the ANOSIM metric, and confronted with other potential groupings, shown in Suppl. Table 1.

Dataset	Groups	ANOSIM
All	Starting vs Final	0.029
All	Parent+Children	0.656
Starting	Classes	0.643
Final	Replicates	0.004
Final	Classes	0.780
Final	Children	0.716
Replicate 1	Classes	0.707
Replicate 2	Classes	0.793
Replicate 3	Classes	0.784
Replicate 4	Classes	0.839

Starting communities		
Class	Number	
1	91	
2	18	
3	70	
4	86	
5	10	

Final communities		
Replica	Class	Number
1	1	209
1	2	66
2	1	195
2	2	80
3	1	190
3	2	85
4	1	200
4	2	75

Table 1: **Classes statistics.** (Top) ANOSIM values obtained by subsetting and dividing the data into different groups. The term 'Parent' refers to each of the 275 starting communities and 'Children' to their four revived replicates. Therefore, 'Parent+Children' means each of the 275 groups comprising each parent and its children and 'Children' to the same classification excluding parents. (Bottom) Number of communities for starting and final classes.

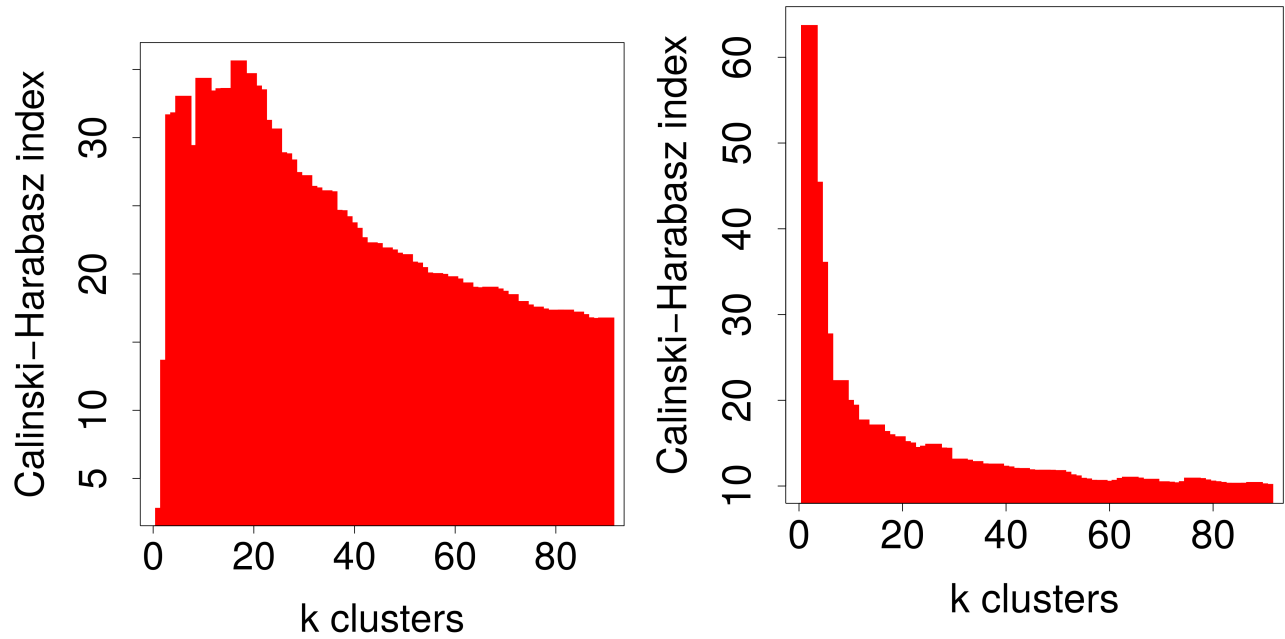


Figure 4: **Determination of number of community classes.** Communities were clustered according to their Jensen-Shannon distance using a partition-around-medoids clustering for an increasing number of clusters  $k$  ( $x$ -axis), and the Calinski-Harabasz index computed to estimate the optimal clustering. (Left) Starting communities have an absolute maximum when communities are classified in 17 clusters. In previous work, we worked with the same communities defined by Operational Taxonomic Units finding a maximum at 6 clusters, which means that ASVs allow us to identify a higher variability. For consistency with previous work, here we also work with the classification in 6 clusters, which corresponds to the second maximum. (Right) Final communities have an absolute maximum when communities are classified in 2 clusters. Results are for replicate 1. The other three replicates are similar.

## Supplementary Note 2. Landscape transformation and equivalent classes

Since the four replicates of final communities had their optimal classification for two clusters, we asked if these classes were equivalent across replicates. To answer this question, we computed all-against-all Jensen-Shannon distances between all samples, i.e. including starting communities and the four replicates of final communities. We then computed the mean distance within each class and between classes, which were determined independently for each dataset. We found that the first (second) class of final communities were more similar among themselves than they were with respect to the second (first) class found in their own replicate, suggesting that the classifications were equivalent (Suppl. Fig. 7). Interestingly, starting community classes 1 and 4 (containing the largest set of communities) were clustered with final community class 1 and have a high similarity, suggesting that it is a large stable attractor. On the other hand, starting community classes 2, 3 and 5 clustered with the final community class 2, but their mean similarity is much lower, suggesting that the new attractor represented by final community class 2 demands a more marked transformation in the starting community composition.

The transformation of the compositional landscape is illustrated in Suppl. Fig. 5, together with other potential scenarios. The dependence of the trajectories from starting classes membership is shown in Fig. 6.

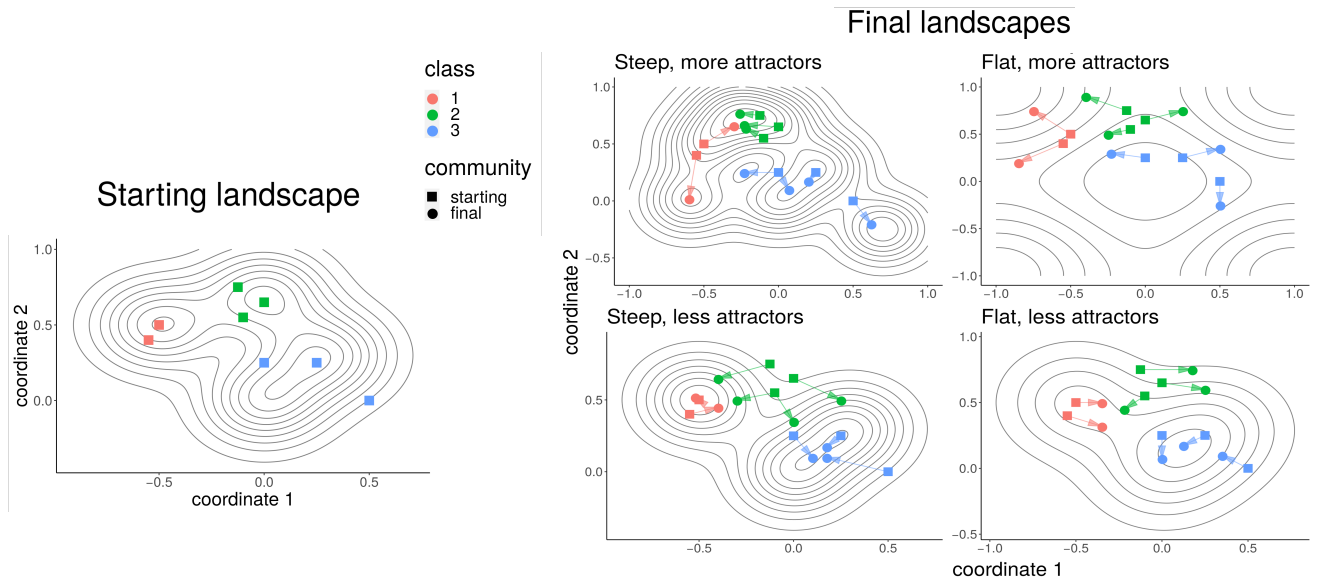


Figure 5: **Transformation of the compositional landscape.** Illustration showing an imaginary transformation in which a starting landscape can be transformed into one of four possible hypothetical final landscapes. (Left) Illustration of the compositional landscape from the perspective of the starting communities. Three attractors corresponding to three community classes are shown, with squares representing the starting communities. (Right) Four hypothetical final landscapes showing an increase/decrease in the number of attractors and the slope of the landscape with respect to the initial landscape. The trajectories of the initial communities depend on the initial positions relative to the final landscape. Our results are described by a scenario in which the number of attractors is reduced, with one of them (Final Class 1) being steep and Final Class 2 possibly flat.



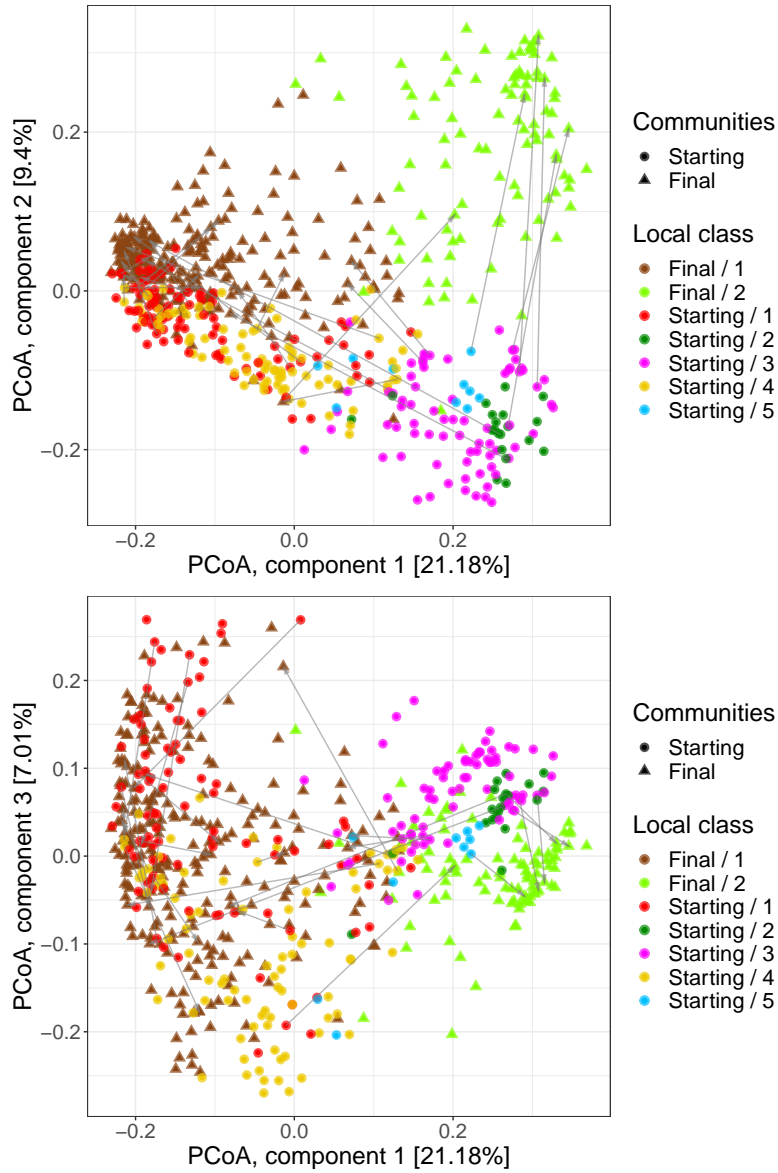


Figure 6: **Correspondence between starting and final classes.** PCoA of the starting- and final communities for one of the replicates showing the correspondence between the starting community and the two final community classes for components 1 and 2 (top) and 1 and 3 (bottom). We observed that the number of attractors was reduced and that the topography likely flattened because the points became more dispersed, especially for final class 2. A random subset (10%) of the trajectories are shown using arrows.

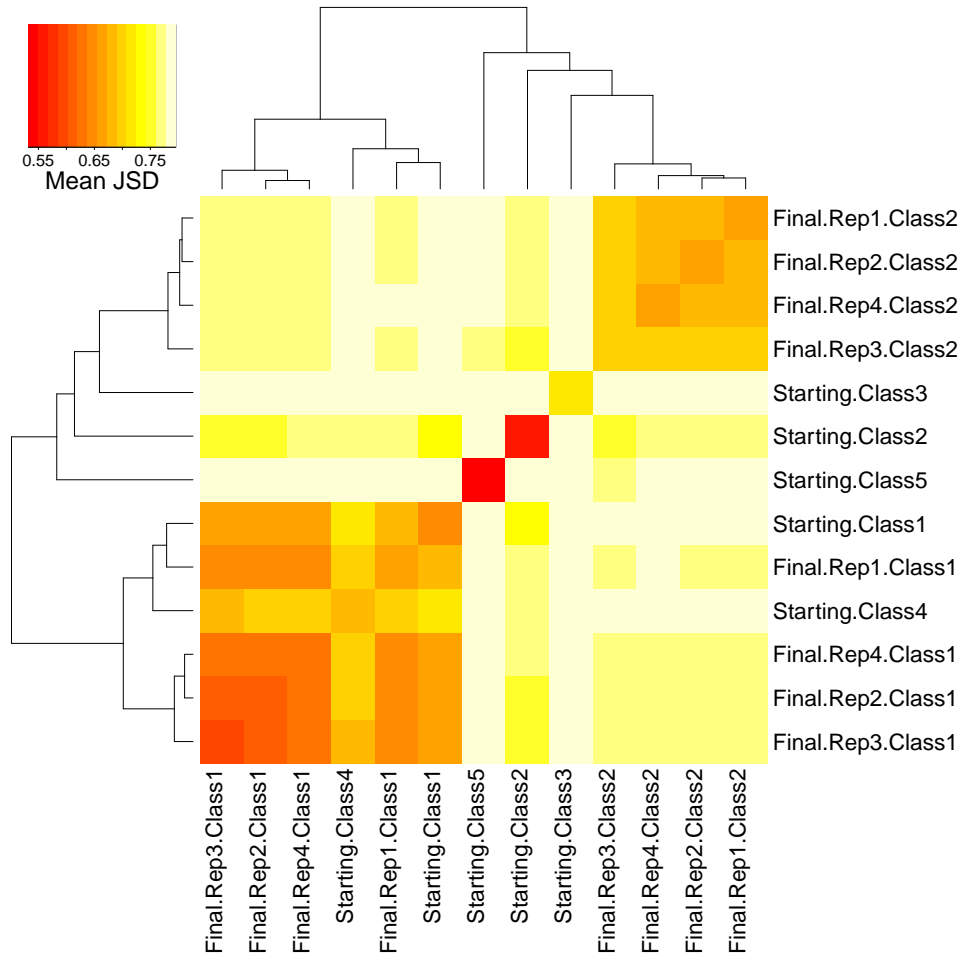


Figure 7: **Similarity between community classes.** Heatmap showing the mean Jensen-Shannon diversity between communities belonging to different classes (starting communities, labeled starting, and the four replicates of the final communities, labeled final). Starting community classes 1 and 4 cluster with the four replicates of final community classes 1. Final community class 2 also cluster together, with starting community class 2 being the more similar one. Starting community class 3 and 5 are the most dissimilar to any other class.

### Supplementary Note 3. Relative abundances change of ASVs propensities' groups

We found a set of cosmopolitan species, namely those with significant propensities for the three types of trajectories at both time points, whose relative abundances tended to be below 0.2 for communities converging to class 1 at the beginning of the experiment (Fig. 8a vertical dotted line) and below this value (around 0.125) at the end of the experiment (horizontal dotted line). Note that propensities were computed on the basis of their presence-absence throughout all communities and, hence, relative abundances were not used in the computation.

A notable proportion of ASVs (23.6%) had a propensity to converge to class 1 at the beginning of the experiment, but not at the end of the experiment (Fig. 8b). Conversely, 21% of ASVs had no significant propensity at the beginning of the experiment, but converged to class 1 at the end (Fig. 8b). This result is not just a simple consequence of ASVs that were not revived (were at high abundance at the start but declined significantly by the end). Although ASVs that declined in abundance over the experiment may have had some influence, they represented only ~3% of all reads while, in some communities, revived ASVs whose abundances were reduced sometimes had total relative abundances as high as 0.7 at the beginning of the experiment (Fig. 8c).

Taking together these results and those presented in Main Text we observed that communities converging to final class 1 had associated a large fraction of ASVs (that possibly were sorted in the first experiment or earlier in their native environment, see (1)). While approximately half of them consistently travelled to the final state, there was another set of ASVs that was excluded, and another set of approximately the same number of ASVs than the one excluded that was co-selected. Our results showed that a coarse-grained description that focuses on sets of ASVs provided valuable insights in the dynamical behaviour of complex microbial communities.

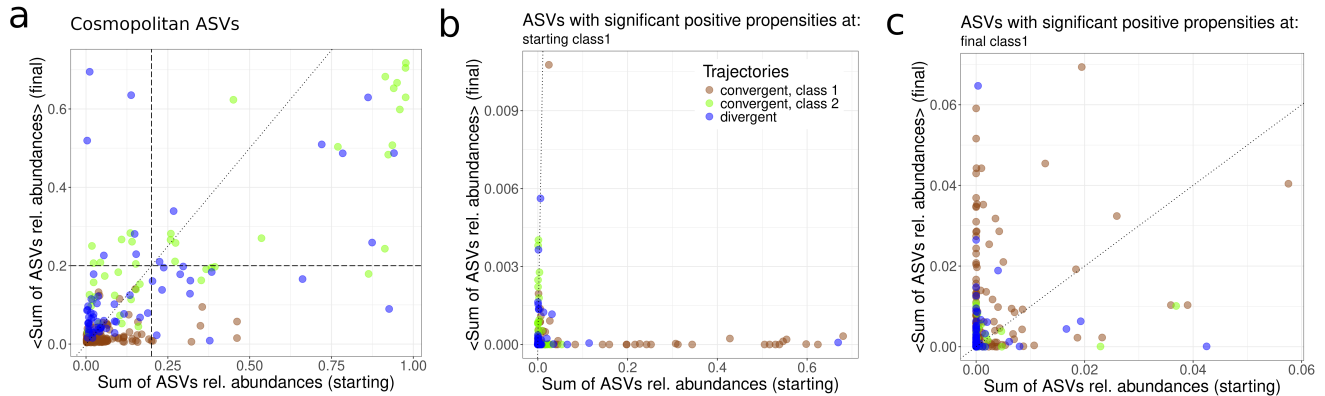


Figure 8: **Change in the relative abundances of groups of ASVs.** Sum of the relative abundances of (a) ASVs belonging to the cosmopolitan group, (b) ASVs having a propensity to class 1 at the beginning of the experiment, and (c) having a propensity to class 1 at the end of the experiment. The figure compares this sum in starting vs. final experiments for each community (averaged across replicates for final communities). Communities were coloured according to the type of trajectory in which they were classified.

## Supplementary Note 4. Statistical analysis of metagenomics predictions

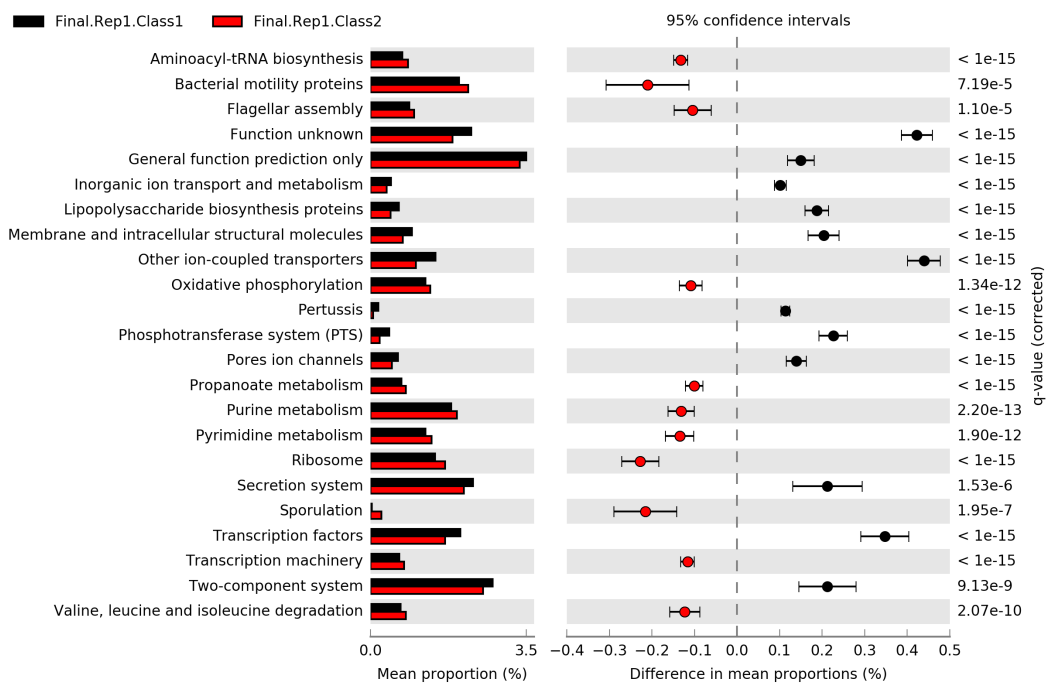


Figure 9: **Example of statistical test for the analysis of metagenome pathways.** Rows indicate KEGG pathways found significant in the comparison between class 1 and class 2 of final communities (first replicate). The first column is the mean proportion of each class, the second column the difference in mean proportions and the third column the Benjamini-Hochberg corrected p-value (termed q-value) of a Welch's test. Only pathways with a difference larger than 0.1 are shown. Significant pathways found in the comparison between class 1 and class 2 for each replicate were used to create the heatmap shown in the Main Text.

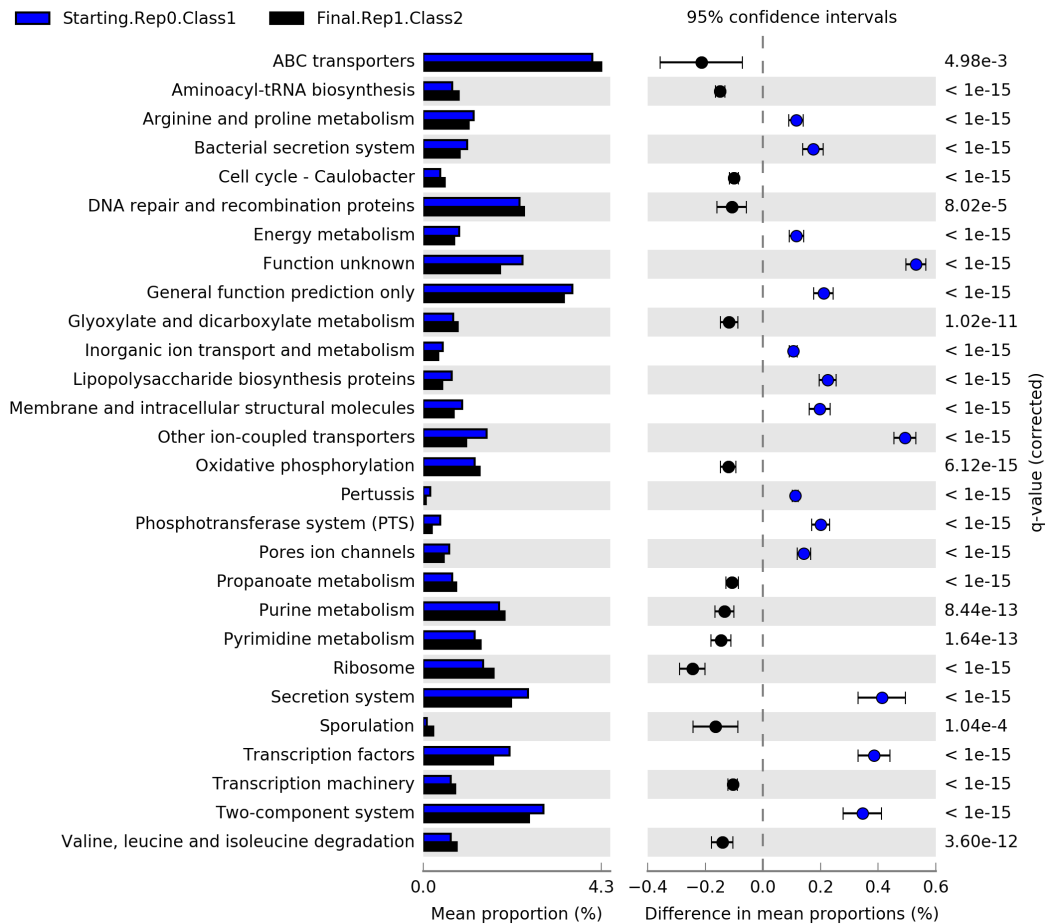


Figure 10: **Example of statistical test for the analysis of metagenome pathways.** Rows indicate KEGG pathways found significant in the comparison between starting communities class 1 and final communities class 2 (first replicate). The first column is the mean proportion of each class, the second column the difference in mean proportions and the third column the Benjamini-Hochberg corrected p-value (termed q-value) of a Welch's test. Only pathways with a difference larger than 0.1 are shown. Significant pathways found in these comparisons were used to create the heatmap shown in Suppl. Fig 11.

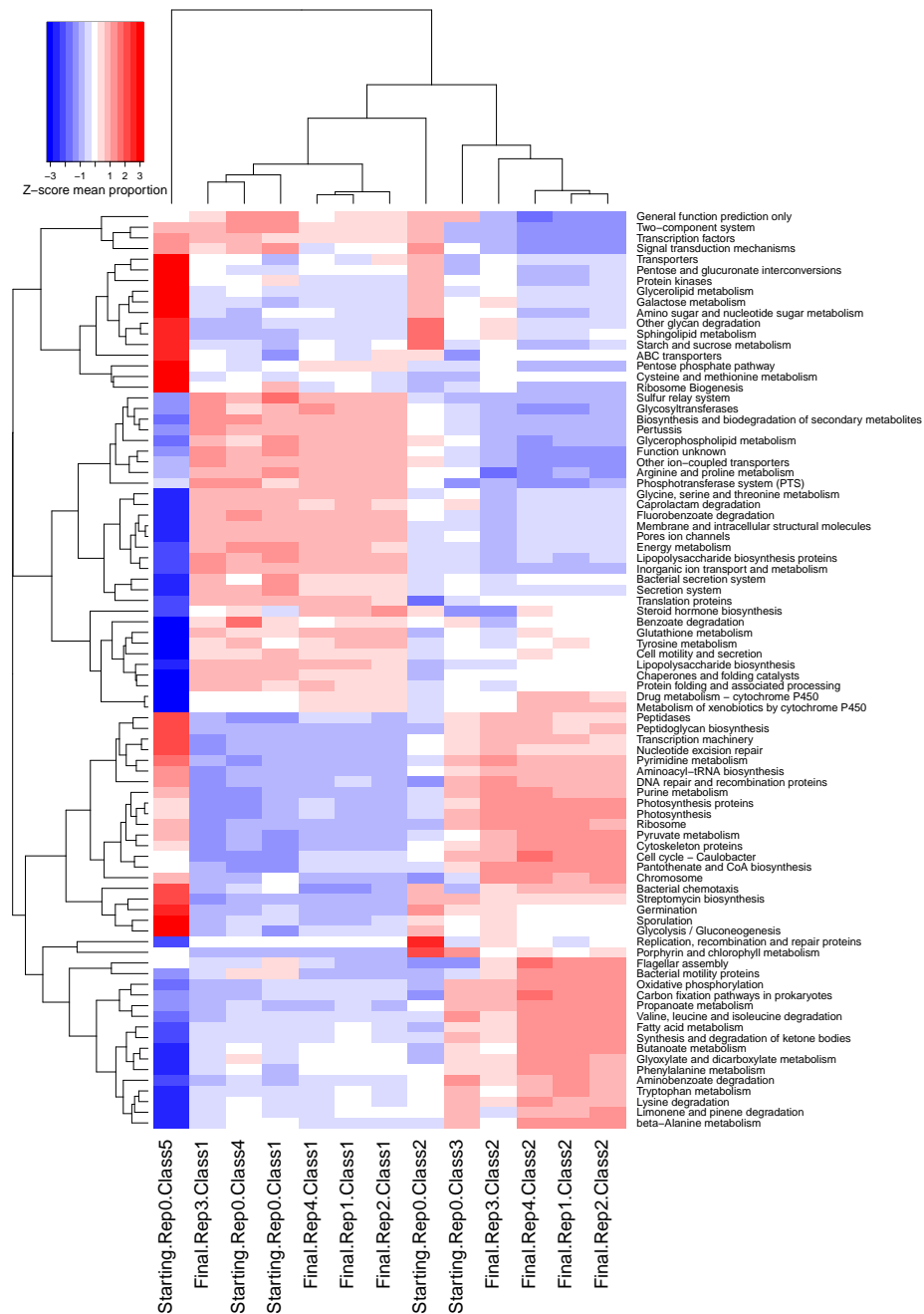


Figure 11: **Metagenomic convergence.** Z-score of the difference in mean proportions of genes clustered in KEGG metabolic pathways between starting- and final community classes. The scaling of the Z-score was computed for each pathway (i.e. scaled by rows), and only pathways showing a significant difference are shown (Welch test corrected for multiple testing). Clustering of classes is similar to the compositional clustering shown in Fig. 7, with starting classes 1 and 4 joining final class 1, while final class 2 cluster independently. Starting community classes 2 and 3 appear intermediate between both. Starting class 5 seems to be an outlier, with very significant pathways. This means that its communities are functionally very similar but note, however, that this class hosts the lowest number of communities (only 10).

## References

1. Pascual-García A, Bell T. **Community-level signatures of ecological succession in natural bacterial communities.** *Nature communications.* 2020;11(1):1–11.